

X-ray absorption spectroscopy of a coordinatively unsaturated 3d transition metal complex

Cite as: *J. Chem. Phys.* **163**, 171103 (2025); doi: [10.1063/5.0303651](https://doi.org/10.1063/5.0303651)

Submitted: 23 September 2025 • Accepted: 21 October 2025 •

Published Online: 5 November 2025











View Online



Export Citation



CrossMark

Meiyuan Guo,¹  Timo Dederichs,²  Lucia Enzmann,^{3,a)}  Ambar Banerjee,⁴  Vicente Zamudio-Bayer,⁵ 
Marcus Lundberg,^{1,b)}  Philippe Wernet,^{2,c)}  and Raphael M. Jay^{2,d)} 

AFFILIATIONS

¹ Department of Chemistry—Ångström Laboratory, Uppsala University, 751 20 Uppsala, Sweden

² Department of Physics and Astronomy, Uppsala University, 751 20 Uppsala, Sweden

³ Physikalisches Institut, Universität Heidelberg, 69120 Heidelberg, Germany

⁴ Research Institute for Sustainable Energy (RISE), TCG Centres for Research and Education in Science and Technology (TCG-CREST), Kolkata 700091, India

⁵ Abteilung für Hochempfindliche Röntgenspektroskopie, Helmholtz-Zentrum Berlin für Materialien and Energie, 12489 Berlin, Germany

^{a)} Present address: Max Planck Institute for Nuclear Physics, 69029 Heidelberg, Germany.

^{b)} Electronic mail: marcus.lundberg@kemi.uu.se

^{c)} Electronic mail: philippe.wernet@physics.uu.se

^{d)} Author to whom correspondence should be addressed: raphael.jay@physics.uu.se

ABSTRACT

Coordinatively unsaturated transition-metal complexes are employed as active catalysts in a wide range of homogeneous chemical reactions, including C–H bond activation. Because of their high reactivity and resulting affinity to rapidly bind substrate molecules, they are generally challenging to detect and characterize when prepared photochemically. Here, we generate the 16-electron cationic complex $[\text{CpFe}(\text{CO})_2]^+$ (Cp = cyclopentadienyl) in the gas phase using electrospray ionization and probe its electronic structure with x-ray absorption spectroscopy at the Fe L-edge. Supported by multiconfigurational spectrum calculations, the distinct L-edge absorption profile of $[\text{CpFe}(\text{CO})_2]^+$ reveals direct access to a low-lying unoccupied Fe 3d-derived orbital, which is characteristic of the unsaturated coordination of the complex and of its pronounced affinity to bind even notoriously unreactive moieties such as alkanes.

© 2025 Author(s). All article content, except where otherwise noted, is licensed under a Creative Commons Attribution-NonCommercial 4.0 International (CC BY-NC) license (<https://creativecommons.org/licenses/by-nc/4.0/>). <https://doi.org/10.1063/5.0303651>

Transition-metal complexes with a nominal count of 16 valence electrons play a decisive role as intermediates in a wide range of homogeneous catalytic reactions. Processes such as alkene hydrogenation and hydroformylation, as well as various carbon–carbon and carbon–heteroatom cross-coupling reactions,¹ all involve the detachment of a ligand from a coordinatively saturated (18-electron) precatalyst to produce a highly reactive 16-electron species with a catalytically active binding site at the metal center. This enables such systems to even bind inert noble gas atoms² as well as highly unreactive nonpolar molecules such as saturated hydrocarbons (e.g., methane or longer-chain alkanes).^{3–5} In this way, 16-electron species also play a decisive role as intermediates in a wide range of C–H bond activation reactions.^{6,7}

In recent years, cationic 16-electron complexes of the form $[\text{CpM}(\text{CO})_2]^+$ (Cp = cyclopentadienyl, M = Fe, Ru, Os) have been shown to be particularly useful in this regard.^{8–10} For this class of systems, UV irradiation of the tricarbonyl $[\text{CpM}(\text{CO})_3]^+$ parent complexes can be used to create the coordinatively unsaturated $[\text{CpM}(\text{CO})_2]^+$ dicarbonyl complex via the dissociation of a CO ligand (see Fig. 1). This 16-electron species is then capable of rapidly binding even notoriously unreactive chemical moieties such as alkane C–H bonds when dissolved in an alkane-saturated 1,1,1,3,3,3-hexafluoropropane solution, thus recovering a nominal 18-electron configuration. However, it is important to note that the 16-electron $[\text{CpM}(\text{CO})_2]^+$ intermediates could not be detected experimentally and were only indirectly inferred.^{8–10} This is a direct

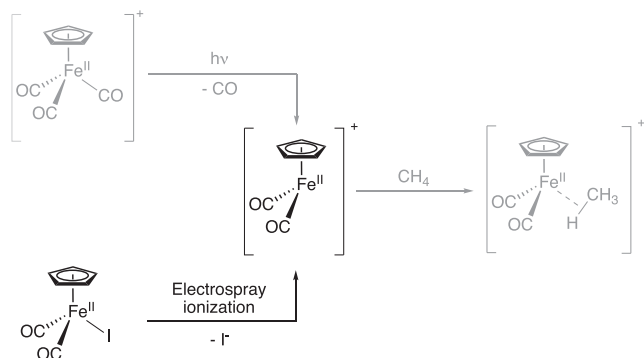


FIG. 1. Schematic depiction of the generation of $[\text{CpFe}(\text{CO})_2]^+$ using conventional photochemical routes as well as electro spray ionization used here.

consequence of their high reactivity, which constitutes a fundamental prerequisite for their application in C–H bond activation and other homogeneous reactions but also renders 16-electron systems elusive, short-lived intermediates that are typically challenging to detect and characterize in experiments.

Pump–probe measurements have been successful in experimentally detecting coordinatively unsaturated 16-electron species that were prepared via photoinduced ligand dissociation, both in the gas phase^{11–17} and in solution.^{18–27} However, the lifetimes of these systems are typically on the order of hundreds of femtoseconds to a few picoseconds before the complexes, when placed in a solution environment, bind to incoming solvent molecules.^{18–27} In the gas phase, where excess vibrational energy cannot be dissipated to the solvent environment, 16-electron complexes instead often further dissociate.^{11–17} Typical lifetimes of photoproducted 16-electron complexes measured in pump–probe experiments are therefore in the same range as typical timescales of vibrational cooling and excited-state dynamics. In addition, because of the limited photolysis yield in pump–probe experiments, transient spectroscopic fingerprints of 16-electron photoproducts must be recorded against a background of unexcited parent complexes. Consequently, in-depth spectroscopic investigations of the electronic structure of 16-electron complexes have thus far been challenging.

Here, we therefore choose a different approach by preparing $[\text{CpFe}(\text{CO})_2]^+$ using electro spray ionization²⁸ (see Fig. 1) and trapping the stable complex in the gas phase for spectroscopic characterization. Using X-ray absorption spectroscopy (XAS) at the metal L-edge,^{23,26,27,29} we directly probe and characterize the valence electronic structure of the system locally around the metal center via dipole-allowed Fe 2p \rightarrow 3d transitions. In combination with multiconfigurational spectrum calculations, we thus present a detailed analysis of the manifold of unoccupied 3d-derived orbitals that determine the high reactivity of $[\text{CpFe}(\text{CO})_2]^+$ and related 16-electron complexes.

The experiments were carried out at the Ion Trap endstation³⁰ located at the UE52-PGM beamline of the BESSY II synchrotron operated by Helmholtz-Zentrum Berlin für Materialien und Energie. Details of the experimental setup were previously reported elsewhere.^{31,32} In short, $[\text{CpFe}(\text{CO})_2]^+$ ions were produced by spraying ~ 1 mM solutions of commercially available

$\text{CpFe}(\text{CO})_2\text{I}$ in methanol. $[\text{CpFe}(\text{CO})_2]^+$ ions are then mass selected using a quadrupole mass filter and stored in a radio-frequency ion trap for accumulation and thermalization at ~ 20 K via a cryogenic helium buffer gas.

Figure 2 shows the experimental x-ray absorption spectrum of $[\text{CpFe}(\text{CO})_2]^+$ recorded at the Fe L-edge. The spectrum was acquired by recording the partial ion yield of Fe^+ ions as a function of the incident photon energy. The production of Fe^+ ions constituted the fragmentation channel with the highest ion yield across the Fe L-edge. Partial ion-yield spectra based on other fragments, which were produced at lower ion yields, result in equivalent spectral shapes; however, at substantially reduced signal-to-noise ratios (see the supplementary material). The L_3 -edge absorption spectrum of $[\text{CpFe}(\text{CO})_2]^+$ exhibits three distinct absorption resonances at incident photon energies of ~ 707 , ~ 709 , and ~ 712 eV. At the L_2 -edge in the photon energy range between 719 and 727 eV, this structure is repeated; however, the first two resonances are merged due to the increased lifetime broadening and reduced energetic splitting. It is important to note that this spectral behavior with three distinct absorption resonances at the L_3 -edge is strikingly different compared to other nominal Fe^{II} singlet complexes involving high-field back-donating ligands such as Cp, CN^- , and CO groups.^{33–37} This can be directly observed by comparing the L_3 -edge absorption spectrum of $[\text{CpFe}(\text{CO})_2]^+$ to the spectra of ferrocene³³ and ferrocyanide,³⁴ as well as $[\text{Fe}(\text{PaPy}_3)\text{CO}]^+$ [$\text{PaPy}_3 = \text{N,N-bis(2-pyridylmethyl)amine-N-ethyl-2-pyridine-2-carboxamide}$],³⁵ which are additionally shown in Fig. 2. At the L_3 -edge, the latter three spectra exhibit only two main absorption resonances, whose origins are well-established.^{33–35,38} Within the framework of pseudo-octahedral symmetry, the first resonance results from the core-excitation of

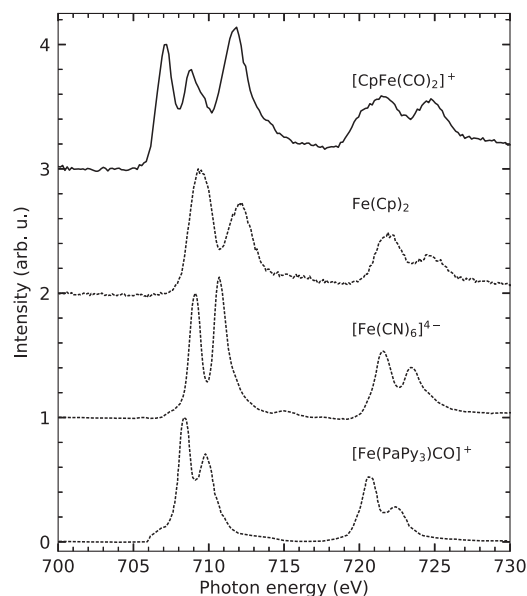


FIG. 2. Experimental Fe L-edge absorption spectrum of $[\text{CpFe}(\text{CO})_2]^+$ (a schematic depiction of its molecular structure is additionally shown) compared to the spectra of ferrocene $[\text{Fe}(\text{Cp})_2]$, gas phase,³³ ferrocyanide $[\text{Fe}(\text{CN})_6]^{4-}$, powder,³⁴ and $[\text{Fe}(\text{PaPy}_3)\text{CO}]^+$ (powder).³⁵

Fe 2p electrons into mainly Fe 3d(e_g)-derived orbitals. The second resonance exhibits similar Fe 3d(e_g) character but also contains substantial contributions from core-excitations to ligand- π^* -derived orbitals that adapt substantial oscillator strength due to strong back-donation from the Fe 3d manifold. As all of these systems, in contrast to $[\text{CpFe}(\text{CO})_2]^+$, constitute coordinatively saturated 18-electron systems, it can be directly inferred from this comparison that the impact of an unsaturated coordination on the electronic structure of the 16-electron complex $[\text{CpFe}(\text{CO})_2]^+$ is directly reflected in an additional peak in its L-edge absorption spectrum. Previous theoretical investigations have suggested that the removal of a ligand from an 18-electron system leads to the substantial stabilization of a single unoccupied metal 3d-derived orbital driven by the loss of the strong anti-bonding interaction with the removed ligand.^{6,39} The Fe L-edge absorption spectrum of $[\text{CpFe}(\text{CO})_2]^+$ suggests that the additional absorption feature at ~ 707 eV is a direct experimental fingerprint of this orbital stabilization.^{23,26,27,29}

To substantiate these purely experimental observations and assign the individual experimentally observed absorption features, Fig. 3(a) shows the experimental Fe L-edge absorption spectrum of $[\text{CpFe}(\text{CO})_2]^+$ compared to a calculated spectrum based on the restricted active space method,^{40–43} with dynamic correlation from multiconfiguration pair-density functional theory (MC-PDFT).^{44–46} The spectrum calculations are performed using OpenMolCAS,⁴⁷ more computational details are available in the [supplementary material](#). The calculated spectrum of $[\text{CpFe}(\text{CO})_2]^+$ in its singlet ground state shows excellent agreement with the experimental spectrum, reproducing all experimentally observed features in terms of peak intensities and relative energies, particularly the three experimentally observed absorption features at the L_3 -edge. The calculations therefore allow for the robust analysis and assignment of the character of the underlying core-excitations. For this, we turn to the spectral analysis in terms of orbital contributions,^{42,48} which is shown in Fig. 3(b). Orbital contributions are derived from the

difference in orbital occupations between the ground state and the core-excited states, correlated with the oscillator strengths of the individual transitions. Consequently, both positive (electron gain) and negative (electron loss) “intensities” are observed.^{42,48} Notably, the electron loss in the Fe 2p core orbital is not depicted, as it consistently involves the loss of a single electron in all cases. All valence orbitals included in the active space of the calculations are shown in Fig. 3(c).

The orbital contribution analysis allows us to robustly assign the first Fe L-edge absorption resonance at ~ 707 eV predominantly to Fe 2p $\rightarrow 3d_{z^2}$ excitations [see Figs. 3(b) and 3(c)] with minor admixture from Fe 2p $\rightarrow 3d_{x^2-y^2}$ excitations as well as multi-electron excitations involving occupied Fe 3d and L(σ) orbitals. The calculations, therefore, clearly confirm that L-edge absorption spectroscopy directly probes the previously hypothesized low-lying unoccupied 3d orbital that is oriented toward the open coordination site^{23,26,27,29,49} [see Fig. 3(c)]. Core excitations beyond the first resonance at ~ 707 eV exhibit a more complex multiconfigurational character. Both features at ~ 709 and ~ 712 eV again exhibit core-excitations into the $3d_{z^2}$ orbital as the leading contribution; however, with substantial admixture from excitations into the $3d_{x^2-y^2}$ orbital [see Figs. 3(b) and 3(c)]. The strong contribution of the $3d_{z^2}$ orbital throughout the whole Fe L-edge is a direct reflection of its low hybridization with ligand-derived orbitals [see Fig. 3(c)], which provides core-excitations into the $3d_{z^2}$ orbital with substantial oscillator strength. Similar to other Fe(II) complexes with strongly back-donating ligands,^{34,35} the resonance at ~ 712 eV additionally shows a significant contribution from excitations into the unoccupied L(π^*) orbitals. Both absorption features at ~ 709 and ~ 712 eV further display a notable occupation decrease of the occupied metal character orbitals $[3d_{xy}$, $3d_{xz}$, and $3d_{yz}]$; see Figs. 3(b) and 3(c)]. This pronounced multiple-electron excitation character can be rationalized by the fact that the resonances at ~ 709 and ~ 712 eV are dominated by heavily mixed triplet and quintet core-excited final states (see spin

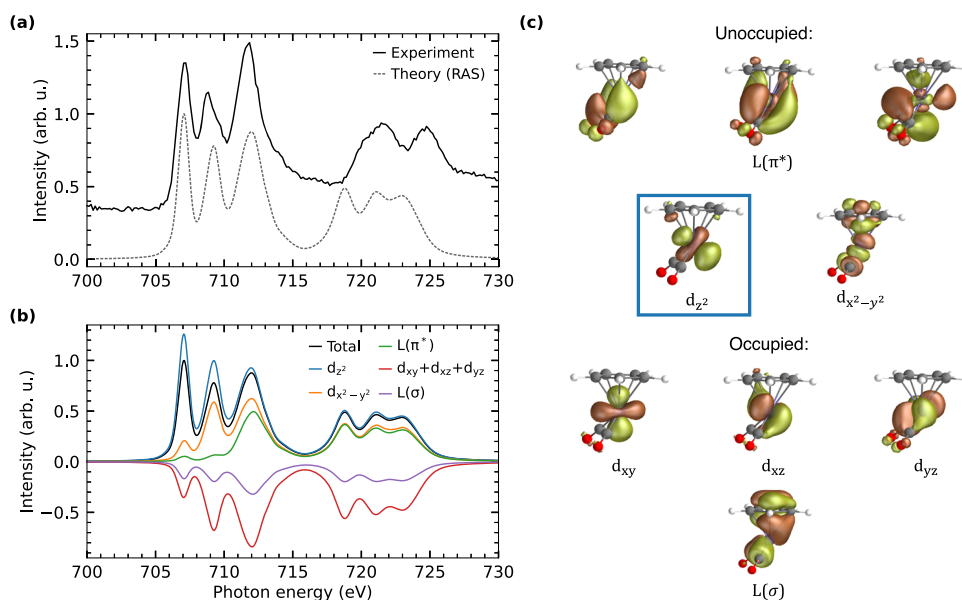


FIG. 3. (a) Experimental L-edge absorption spectrum of $[\text{CpFe}(\text{CO})_2]^+$ compared to simulations calculated at the MC-PDFT level of theory. The calculated Fe L-edge absorption spectrum is scaled to match the intensity of the experimental peak at ~ 707 eV. (b) Decomposition of the calculated Fe L-edge absorption spectrum into contributions from the orbitals of the active space included in the calculations. (c) Plot of the molecular valence orbitals (plotted at an isovalue of 0.05) included in the active space.

decomposition analysis in the [supplementary material](#)), necessitating a change in population in more than one valence orbital in the core-excited final states.

To better understand the spectral impact of the decisive $3d_{z^2}$ orbital, it is instructive to contrast the spectral behavior of $[\text{CpFe}(\text{CO})_2]^+$ with Fe L-edge calculations of its nominal parent complex $[\text{CpFe}(\text{CO})_3]^+$, shown in [Fig. 4\(a\)](#). As a coordinately saturated singlet 18-electron system with strong back-donation ligands and an approximately pseudo-octahedral geometry, $[\text{CpFe}(\text{CO})_3]^+$ displays spectral features similar to those of ferrocene, ferrocyanide, and $[\text{Fe}(\text{PaPy}_3)\text{CO}]^+$, shown in [Fig. 2](#). The two characteristic resonances of such systems can be observed, both dominated by excitations into unoccupied $3d(e_g)$ orbitals, with the second resonance further exhibiting substantial $L(\pi^*)$ admixture [see orbital decomposition analysis of $[\text{CpFe}(\text{CO})_3]^+$ in the [supplementary material](#)]. To track how this spectral behavior evolves upon the gradual removal of one CO ligand, [Fig. 4\(a\)](#) additionally shows calculated Fe L-edge absorption spectra for structures in which one Fe–CO bond is incrementally elongated with respect to the optimized structure of singlet $[\text{CpFe}(\text{CO})_3]^+$ (while all other atoms remain fixed). A small elongation (0.2 Å) leads to a shift of the $3d(e_g)$ resonance to lower energy, consistent with a reduced ligand field.³⁶ Further

elongation of Fe–CO distances (0.4 Å) leads to a broadening of the resonance, which ultimately evolves into a separate absorption resonance at an elongation beyond 0.6 Å. At the same time, the intensity of the resonance near ~ 712 eV decreases progressively, reflecting a reduction in Fe–CO back-donation, in agreement with previous observations of photoinduced ligand-exchange dynamics in metal carbonyl and cyanide complexes.^{26,27,50} Interestingly, the intermediate structure with an Fe–CO bond elongated by 0.4 Å exhibits a spectral profile that closely resembles the Fe L-edge absorption spectrum of the $[\text{CpFe}(\text{CO})_2]_2$ dimer,⁵¹ where two of the four CO ligands are shared between the iron centers, which leads to an increased Fe–CO distance compared to the terminal CO ligand.⁵²

The dominant impact of CO removal on the valence electronic structure in generating an undercoordinated 16-electron complex is illustrated in [Fig. 4\(b\)](#). It shows the evolution of the orbital energy difference between the $3d_{z^2}$ and $3d_{x^2-y^2}$ orbitals upon step-wise elongation of a CO ligand in $[\text{CpFe}(\text{CO})_3]^+$ (details of the relative orbital energy difference calculations can be found in the [supplementary material](#)). Consistent with the pseudo-octahedral coordination environment of $[\text{CpFe}(\text{CO})_3]^+$, these two orbitals are nearly degenerate $3d(e_g)$ -like orbitals. This degeneracy is progressively lifted upon elongation of the Fe–CO bond, resulting in a splitting of the $3d(e_g)$ manifold into the now energetically distinct $3d_{z^2}$ and $3d_{x^2-y^2}$ orbitals. The splitting is primarily driven by a substantial decrease in energy of the $3d_{z^2}$ orbital, which loses one strong anti-bonding interaction with the dissociating CO ligand. Spectroscopically, this splitting and orbital stabilization can then be directly observed by the emergence of the additional characteristic x-ray absorption resonance at ~ 707 eV in the $[\text{CpFe}(\text{CO})_2]^+$ complex [see [Fig. 4\(a\)](#)]. With L-edge absorption spectroscopy, we can thus directly probe the decisive $3d_{z^2}$ orbital, which, due to its orientation [see [Fig. 3\(c\)](#)] and low energy, serves as an unoccupied orbital with exceptional σ -accepting capabilities.⁶ It is this orbital—coined a “localized hole on the metal” by Roald Hoffmann⁵³—which consequently renders $[\text{CpFe}(\text{CO})_2]^+$ and analogous 16-electron complexes strong Lewis acids³⁹ that are capable of functioning as highly reactive catalysts in a wide range of homogeneous chemical reactions.

In summary, we use a combination of x-ray absorption spectroscopy at the metal L-edge with multiconfigurational calculations to characterize the valence-electronic structure of $[\text{CpFe}(\text{CO})_2]^+$, a prototypical coordinately unsaturated 16-electron transition-metal complex. The experimental data show a unique spectral profile that can be directly attributed to a distinct orbital splitting in the unoccupied manifold of the complex. In agreement with previous theoretical investigations,^{6,39} this splitting is identified as the main reason for the high reactivity of $[\text{CpFe}(\text{CO})_2]^+$ and its ability to bind even quasi-inert chemical moieties such as alkanes.⁹ Our in-depth spectroscopic characterization was made possible by avoiding conventional photochemical approaches in producing 16-electron complexes and instead directly preparing them as stable species in the gas phase via electrospray ionization. This approach thereby paves the way for systematic studies of elusive reaction intermediates that, owing to their extreme reactivity and short lifetimes in homogeneous environments, would otherwise remain inaccessible to detailed spectroscopic investigations.

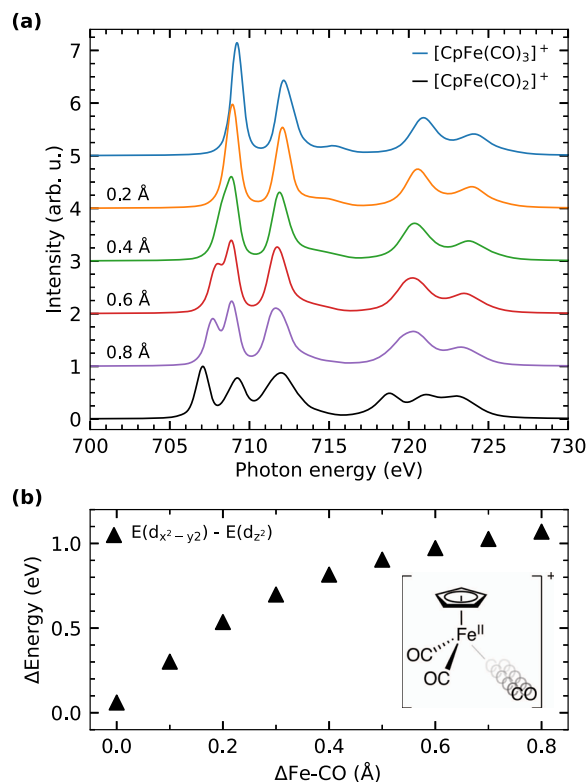


FIG. 4. (a) Calculated Fe L-edge absorption spectrum of $[\text{CpFe}(\text{CO})_3]^+$ compared to calculated spectra of structures with elongated Fe–CO bond lengths as well as of the $[\text{CpFe}(\text{CO})_2]^+$ complex, where the CO is fully removed. (b) Energy difference between the $d_{x^2-y^2}$ and d_{z^2} orbitals as a function of increasing Fe–CO bond distances along the removal of a CO ligand from the $[\text{CpFe}(\text{CO})_3]^+$ parent complex.

The [supplementary material](#) encompasses additional experimental and computational details, spin decomposition analysis, and orbital decomposition analysis of $[\text{CpFe}(\text{CO})_3]^+$.

The authors acknowledge the Helmholtz-Zentrum Berlin für Materialien und Energie for the allocation of synchrotron radiation beamtime. M.G. and M.L. acknowledge funding from the Swedish Research Council under Grant Agreement No. 2022-04794. P.W. acknowledges funding from the Swedish Research Council under Grant Agreement Nos. 2024-05246 and 2019-06093. R.M.J. acknowledges funding from the Swedish Research Council under Grant Agreement No. 2024-03901. The computations were enabled by resources (Grant Nos. NAISS 2024/22-1161, NAISS2025-22-786, NAISS2025-5-435, UPPMAX 2025-2-95, and UPPMAX 2025-2-10) provided by the National Academic Infrastructure for Supercomputing in Sweden (NAISS) and at UPPMAX.

AUTHOR DECLARATIONS

Conflict of Interest

The authors have no conflicts to disclose.

Author Contributions

Meiyuan Guo: Data curation (equal); Formal analysis (equal); Investigation (equal); Methodology (equal); Visualization (equal); Writing – original draft (equal); Writing – review & editing (equal). **Timo Dederichs:** Formal analysis (equal); Investigation (equal); Visualization (equal); Writing – review & editing (equal). **Lucia Enzmann:** Data curation (equal); Formal analysis (equal); Investigation (equal); Writing – review & editing (equal). **Ambar Banerjee:** Investigation (equal); Writing – review & editing (equal). **Vicente Zamudio-Bayer:** Investigation (equal); Methodology (equal); Writing – review & editing (equal). **Marcus Lundberg:** Formal analysis (equal); Investigation (equal); Methodology (equal); Supervision (equal); Writing – review & editing (equal). **Philippe Wernet:** Conceptualization (equal); Formal analysis (equal); Investigation (equal); Supervision (equal); Writing – review & editing (equal). **Raphael M. Jay:** Conceptualization (lead); Formal analysis (equal); Investigation (lead); Methodology (equal); Supervision (equal); Visualization (equal); Writing – original draft (lead).

DATA AVAILABILITY

The data that support the findings of this study are available from the corresponding author upon reasonable request.

REFERENCES

- J. F. Hartwig, *Organotransition Metal Chemistry: From Bonding to Catalysis* (University Science Books, Mill Valley, CA, 2010).
- S. A. Bartlett, N. A. Besley, A. J. Dent, S. Diaz-Moreno, J. Evans, M. L. Hamilton, M. W. D. Hanson-Heine, R. Horvath, V. Manici, X.-Z. Sun, M. Towrie, L. Wu, X. Zhang, and M. W. George, *J. Am. Chem. Soc.* **141**, 11471 (2019).
- C. Hall and R. N. Perutz, *Chem. Rev.* **96**, 3125 (1996).
- A. Cowan and M. George, *Coord. Chem. Rev.* **252**, 2504 (2008).

- A. S. Weller, F. M. Chadwick, and A. I. McKay, “Transition metal alkane-sigma complexes,” in *Advances in Organometallic Chemistry*, 1st ed. (Elsevier Inc., 2016), Vol. 66, pp. 223–276.
- J. Y. Saillard and R. Hoffmann, *J. Am. Chem. Soc.* **106**, 2006 (1984).
- R. G. Bergman, *Nature* **446**, 391 (2007).
- J. D. Watson, L. D. Field, and G. E. Ball, *Nat. Chem.* **14**, 801 (2022).
- J. D. Watson, L. D. Field, and G. E. Ball, *J. Am. Chem. Soc.* **144**, 17622 (2022).
- J. D. Watson, D. Mizdrak, L. D. Field, and G. E. Ball, *Chem. Sci.* **16**, 8532 (2025).
- S. A. Trushin, W. Fuss, W. E. Schmid, and K. L. Kompa, *J. Phys. Chem. A* **102**, 4129 (1998).
- S. A. Trushin, W. Fuss, K. L. Kompa, and W. E. Schmid, *J. Phys. Chem. A* **104**, 1997 (2000).
- W. Fuß, S. A. Trushin, and W. E. Schmid, *Res. Chem. Intermed.* **27**, 447 (2001).
- P. Wernet, T. Leitner, I. Josefsson, T. Mazza, P. S. Miedema, H. Schröder, M. Beye, K. Kunnus, S. Schreck, P. Radcliffe, S. Düsterer, M. Meyer, M. Odelius, and A. Föhlisch, *J. Chem. Phys.* **146**, 211103 (2017).
- T. Leitner, I. Josefsson, T. Mazza, P. S. Miedema, H. Schröder, M. Beye, K. Kunnus, S. Schreck, S. Düsterer, A. Föhlisch, M. Meyer, M. Odelius, and P. Wernet, *J. Chem. Phys.* **149**, 044307 (2018).
- N. C. Cole-Filipiak, J. Troß, P. Schrader, L. M. McCaslin, and K. Ramasesha, *J. Chem. Phys.* **156**, 144306 (2022).
- J. Troß, J. E. Arias-Martinez, K. Carter-Fenk, N. C. Cole-Filipiak, P. Schrader, L. M. McCaslin, M. Head-Gordon, and K. Ramasesha, *J. Am. Chem. Soc.* **146**, 22711 (2024).
- A. G. Joly and K. A. Nelson, *Chem. Phys.* **152**, 69 (1991).
- T. P. Dougherty and E. J. Heilweil, *Chem. Phys. Lett.* **227**, 19 (1994).
- T. Lian, S. E. Bromberg, H. Yang, G. Proulx, R. G. Bergman, and C. B. Harris, *J. Am. Chem. Soc.* **118**, 3769 (1996).
- T. Lian, S. E. Bromberg, M. C. Asplund, H. Yang, and C. B. Harris, *J. Phys. Chem.* **100**, 11994 (1996).
- J. B. Asbury, K. Hang, J. S. Yeston, J. G. Cordaro, R. G. Bergman, and T. Lian, *J. Am. Chem. Soc.* **122**, 12870 (2000).
- P. Wernet, K. Kunnus, I. Josefsson, I. Rajkovic, W. Quevedo, M. Beye, S. Schreck, S. Grübel, M. Scholz, D. Nordlund, W. Zhang, R. W. Hartsock, W. F. Schlotter, J. J. Turner, B. Kennedy, F. Hennies, F. M. F. de Groot, K. J. Gaffney, S. Techert, M. Odelius, and A. Föhlisch, *Nature* **520**, 78 (2015).
- L. Zhu, S. Saha, Y. Wang, D. A. Keszler, and C. Fang, *J. Phys. Chem. B* **120**, 13161 (2016).
- K. Kunnus, I. Josefsson, I. Rajkovic, S. Schreck, W. Quevedo, M. Beye, C. Weniger, S. Grübel, M. Scholz, D. Nordlund, W. Zhang, R. W. Hartsock, K. J. Gaffney, W. F. Schlotter, J. J. Turner, B. Kennedy, F. Hennies, F. M. F. de Groot, S. Techert, M. Odelius, P. Wernet, and A. Föhlisch, *Struct. Dyn.* **3**, 043204 (2016).
- R. M. Jay, A. Banerjee, T. Leitner, R.-P. Wang, J. Harich, R. Stefanik, H. Wikmark, M. R. Coates, E. V. Beale, V. Kabanova, A. Kahraman, A. Wach, D. Ozerov, C. Arrell, P. J. M. Johnson, C. N. Borca, C. Cirelli, C. Bacellar, C. Milne, N. Huse, G. Smolentsev, T. Huthwelker, M. Odelius, and P. Wernet, *Science* **380**, 955 (2023).
- R. M. Jay, M. R. Coates, H. Zhao, M.-O. Winghart, P. Han, R.-P. Wang, J. Harich, A. Banerjee, H. Wikmark, M. Fondell, E. T. J. Nibbering, M. Odelius, N. Huse, and P. Wernet, *J. Am. Chem. Soc.* **146**, 14000 (2024).
- S. Bari, D. Egorov, T. L. C. Jansen, R. Boll, R. Hoekstra, S. Techert, V. Zamudio-Bayer, C. Bülow, R. Lindblad, G. Leistner, A. Ławicki, K. Hirsch, P. S. Miedema, B. von Issendorff, J. T. Lau, and T. Schlathöler, *Chem.-Eur. J.* **24**, 7631 (2018).
- P. Wernet, *Philos. Trans. R. Soc. A* **377**, 20170464 (2019).
- K. Hirsch, J. T. Lau, P. Klar, A. Langenberg, J. Probst, J. Rittmann, M. Vogel, V. Zamudio-Bayer, T. Möller, and B. von Issendorff, *J. Phys. B: At., Mol. Opt. Phys.* **42**, 154029 (2009).
- O. S. Abylasova, M. Guo, V. Zamudio-Bayer, M. Kubin, T. Gitzinger, M. da Silva Santos, M. Flach, M. Timm, M. Lundberg, J. T. Lau, and K. Hirsch, *J. Phys. Chem. A* **127**, 7121 (2023).
- M. Flach, K. Hirsch, T. Gitzinger, M. Timm, M. da Silva Santos, O. S. Abylasova, M. Kubin, B. von Issendorff, J. T. Lau, and V. Zamudio-Bayer, *Inorg. Chem.* **63**, 11812 (2024).
- K. Godehusen, T. Richter, P. Zimmermann, and P. Wernet, *J. Phys. Chem. A* **121**, 66 (2017).

- ³⁴R. K. Hocking, E. C. Wasinger, F. M. F. de Groot, K. O. Hodgson, B. Hedman, and E. I. Solomon, *J. Am. Chem. Soc.* **128**, 10442 (2006).
- ³⁵J. J. Yan, M. A. Gonzales, P. K. Mascharak, B. Hedman, K. O. Hodgson, and E. I. Solomon, *J. Am. Chem. Soc.* **139**, 1215 (2017).
- ³⁶R. M. Jay, S. Eckert, M. Fondell, P. S. Miedema, J. Norell, A. Pietzsch, W. Quevedo, J. Niskanen, K. Kunnus, and A. Föhlisch, *Phys. Chem. Chem. Phys.* **20**, 27745 (2018).
- ³⁷R. M. Jay, V. Vaz da Cruz, S. Eckert, M. Fondell, R. Mitzner, and A. Föhlisch, *J. Phys. Chem. B* **124**, 5636 (2020).
- ³⁸K. Kunnus, W. Zhang, M. G. Delcey, R. V. Pinjari, P. S. Miedema, S. Schreck, W. Quevedo, H. Schröder, A. Föhlisch, K. J. Gaffney, M. Lundberg, M. Odelius, and P. Wernet, *J. Phys. Chem. B* **120**, 7182 (2016).
- ³⁹T. A. Albright, J. K. Burdett, and M.-H. Whangbo, “Five coordination,” in *Orbital Interactions in Chemistry* (John Wiley & Sons, Ltd., 2013), Chap. 17, pp. 465–502.
- ⁴⁰I. Josefsson, K. Kunnus, S. Schreck, A. Föhlisch, F. de Groot, P. Wernet, and M. Odelius, *J. Phys. Chem. Lett.* **3**, 3565 (2012).
- ⁴¹S. I. Bokarev, M. Dantz, E. Suljoti, O. Kühn, and E. F. Aziz, *Phys. Rev. Lett.* **111**, 083002 (2013).
- ⁴²R. V. Pinjari, M. G. Delcey, M. Guo, M. Odelius, and M. Lundberg, *J. Chem. Phys.* **141**, 124116 (2014).
- ⁴³M. G. Delcey, L. K. Sørensen, M. Vacher, R. C. Couto, and M. Lundberg, *J. Comput. Chem.* **40**, 1789 (2019).
- ⁴⁴G. Li Manni, R. K. Carlson, S. Luo, D. Ma, J. Olsen, D. G. Truhlar, and L. Gagliardi, *J. Chem. Theory Comput.* **10**, 3669 (2014).
- ⁴⁵L. Gagliardi, D. G. Truhlar, G. Li Manni, R. K. Carlson, C. E. Hoyer, and J. L. Bao, *Acc. Chem. Res.* **50**, 66 (2017).
- ⁴⁶S. Ghosh, S. Mukamel, and N. Govind, *J. Phys. Chem. Lett.* **14**, 5203 (2023).
- ⁴⁷I. F. Galván, M. Vacher, A. Alavi, C. Angeli, F. Aquilante, J. Autschbach, J. J. Bao, S. I. Bokarev, N. A. Bogdanov, R. K. Carlson, L. F. Chibotaru *et al.*, *J. Chem. Theory Comput.* **15**, 5925 (2019).
- ⁴⁸M. Kubin, M. Guo, M. Ekimova, E. Källman, J. Kern, V. K. Yachandra, J. Yano, E. T. J. Nibbering, M. Lundberg, and P. Wernet, *J. Phys. Chem. B* **122**, 7375 (2018).
- ⁴⁹T. R. Ward, O. Schafer, C. Daul, and P. Hofmann, *Organometallics* **16**, 3207 (1997).
- ⁵⁰V. Vaz da Cruz, E. J. Mascarenhas, R. Büchner, R. M. Jay, M. Fondell, S. Eckert, and A. Föhlisch, *Phys. Chem. Chem. Phys.* **24**, 27819 (2022).
- ⁵¹S. Carlotto, P. Finetti, M. de Simone, M. Coreno, G. Casella, M. Sambri, and M. Casarin, *Inorg. Chem.* **58**, 5844 (2019).
- ⁵²R. F. Bryan and P. T. Greene, *J. Chem. Soc. A* **1970**, 3064.
- ⁵³R. Hoffmann, *Angew. Chem. Int. Ed. Engl.* **21**, 711 (1982).